Analysis of coupling efficiency between the rib waveguide and single mode fibre (SMF)

G. J. D. Collins and S. Haxha
Photonics Group, Department of Electronics, University of Kent, Canterbury

***Abstract* – A study of a new optical mode transformer or spot-size converter (SSC) and optimisation of its parameters is demonstrated. Particular attention is paid to the guiding layer and solutions are sought via full vectorial finite element method to produce the desired profiles for hybrid modes along the lateral axis. Matching of the optical modes (field profiles) between the rib waveguide and single mode fibre (SMF) is presented.**

I. Introduction

Communications Networks have advanced at an alarming rate over the past decade but the hindrance of existing Microelectronic technologies have caused substantial bottlenecks. This is no more apparent than in the long-haul digital backbones and trunk interconnections. The most advanced cabling technology of the era is Fibre Optics, where an ostensibly endless amount of information bandwidth is delivered to the network. Methods of revolutionising established technologies are now available in the guise of Integrated Photonics. Silicon is already established in the world of microelectronics, but recent developments have further reinforced the opinion that Silicon on Insulator (SOI) is the viable commercial platform for lightwave communications [1] [2]. Careful choice in the materials of waveguides ensures that the light is confined to the film via total internal reflection. In this paper the structure used is that of a rib waveguide where a high refractive index contrast between the Silicon (Si) core and the Silica (SiO_2) cladding is apparent, enabling the light to be confined to the core. For an Integrated Optical device to be successful in its manipulation and propagation of light it must be accurately coupled. Tapered Polymer waveguide structures [3] can be used for coupling light between optical waveguides with differing geometries. They have a number of application areas such as for coupling light onto fibre, fibre onto optoelectronic integrated circuitry (OEIC), or coupling between different waveguide structures in a hybrid OEIC. The latter is the area that relates closely to the work carried out in this paper. Each component has a structure that is optimised for its operation. In this paper certain rib geometry parameters are varied in order to ascertain when the mode is no longer confined to the film, thus radiating into the surrounding polymer area. Integrated Optical devices that produce small and asymmetric spot sizes by using direct butt-coupling as much as 90% of the optical power can be lost. This is due to the mismatch between optical field profiles. With the large loss in power there is a definite need for more accurate coupling which can be realised by using the Spot-Size Converters (SSCs). The SSCs [4] are used in many Photonic sub-systems and certain device geometries are assumed in order to reduce the inherent coupling losses. In this paper the full vectorial finite element method has been employed to design and optimise the SSC. In this SSC design the primary guide has been tapered in such way that the optical mode is forced into the surrounding polymer layer, which is designed to have a similar spot-size to that of the Single Mode Fibre (SMF).

II. Numerical Method

In this paper the numerical modelling of the waveguides is performed using a full vectorial FEM to solve Maxwell's wave equation. This method produces eigenmode solutions to a high degree of accuracy and uses tetrahedral computation of the waveguide cross-section. This triangular meshing allows greater accuracy than for a purely quadrilateral meshing approach such as the Finite Difference Method (FDM). The FEM was chosen because of its ability to handle an arbitrary cross-sectional shape and the spatially varying properties of the medium. It is robust, flexible and applicable to a wide variety of applications [5, 6]. The main concern with a purely numerical approach is that of the computational complexity of the problems. For a structure with large dimensions the computation time was noticeably increased in comparison to structures with a small geometry. With the complexity comes a higher price with regards to system requirements in memory and CPU time. The iterative nature of the computation together with the complexity causes the time factor to be considered closely for a structure with large dimensions. Although for the purposes of the geometry sizes in this paper the FEM method was suitable.

Another very important aspect of the FEM numerical analysis is the variable problem space. This has the effect of improving the accuracy of the computation by allowing the mesh to be changed; allocating a finer mesh to smaller features and a coarser mesh to larger features. This was an important aspect during the simulations of these results. Parameter values were ascertained at each iteration of the simulations in order to produce the most accurate results. These were the propagation constant (β), the spot-size area, and $\boldsymbol{H}_x$ and $\boldsymbol{H}_y$ for each of the TE and TM modes.

III. Discussion of Results

The structure investigated in this paper is the rib waveguide device consisting of SOI. Light propagates in the z direction as quasi TM_0 or TE_0 modes which are mainly polarized along the respective x and y axis. These modes propagate at different propagation constants β_{TM} and $\beta_{TE.}$ Within the geometry presented in Fig. 1 there are a number of parameters that were set for the purposes of the simulations. The refractive indices of the structure were kept the same throughout; Silicon, Si taper guide $n_g = 3.4790$, SiO_2 substrate $n_s = 1.45$, and the polymer coating $n_{pol} = 1.5$. In addition the rib height, H_1 and the rib width, W_1 are kept constant at 10µm. The height of the taper, H is set at 6.0 µm throughout, whilst the width of the taper is varied from an initial value of 3 µm down to a final width of 0 µm. The figure shows a TM mode which is confined in the taper at a cross-sectional area of 3.0 µm x 6.0 µm. The taper end then performs the necessary mode matching to the end of the rib, where the cross-sectional area is 10 µm x 10 µm, and the TM mode is confined within. The end of the rib can then be coupled to the SMF as necessary, which has a circular modal profile of between 10 µm x 10 µm. The modal profiles from the output of the rib and the input of the SMF are quite identical in size, which enable sufficient coupling.

The Propagation Constant, β for TE and TM modes is investigated and their variations with the rib width, W are presented in Fig. 2. From W = 0 to 0.5 µm there is a near linear response, where for an increase in W there is a near proportional increase in β for both TE and TM. It can be observed that at around W = 0.2µm the propagation constant starts to increase rapidly and the TE mode is no longer confined just in the taper, it starts to appear in the polymer coating as well. The plot also shows that the TE mode expansion happens at a greater rate than that of TM mode. From W = 0.5µm onwards both TE and TM modes have almost the same values of β up until W = 3.0 µm. From 0.5 µm to 1.0 µm there is a slow decline in values of β until after 1.0 µm, where the values become almost constant. This is because the modes are entirely confined to the Silicon layer.

The spot size area (SS in µm^2) as a function of the rib width W for both TE and TM is shown in Fig. 3. This Fig. shows that the SS area has a slow linear decay from W= 3.0 µm to 0.1µm for both transversal modes. At W = 0.5 µm they decay at a fractional difference where the TE mode decays more slowly, it then starts to rise at W= 0.05 curving off slightly to a SS of 3 µm^2. The TM SS area decreases more quickly to W = 0.05. Between W = 0.05 and 0.0 µm there is a steep increase in SS for both transversal modes and there is a final SS close to the cross-sectional area of the SMF. After this point, below 0.005 µm the response becomes flat, where the SS is constant.

Simulations were performed for $0 < W < 3$ to enable mode solutions for hybrid TE and TM fundamental modes. Initial dimensions of the Si guide are considered to be; W= 3µm, H = 6µm and $\boldsymbol{H}_x$ and $\boldsymbol{H}_y$ nondominant and dominant field profiles for a TE fundamental mode are shown in Fig. 4 (a), and (b), respectively. It can be seen that for TE mode $\boldsymbol{H}_y$ field is dominant, which is completely confined to the Si guiding layer. The $\boldsymbol{H}_x$, and $\boldsymbol{H}_y$ field profiles for TM have also been performed and shown in Fig. 5 (a) and (b), respectively. The dominant field $\boldsymbol{H}_x$, for the TM mode (Fig. 5 (a)) is well confined within the Si guiding layer. Simulations have been carried out at different cross sections in z-direction until W = 0 µm. The height of the primary guide, H is kept equal to 6.0 µm. The key point of this investigation was to find out at what W the mode will appear to the polymer coating. It has been found that at W = 0.2 µm, (shown in Fig. 6 (a) and (b) the TE mode starts to appear to polymer layer before the TM mode, and this has also been confirmed in Fig. 1 and 2, where the propagation constant and SS area are presented. The $\boldsymbol{H}_x$ and $\boldsymbol{H}_y$ field profiles for the TM mode are presented in Fig. 7 (a) and (b). It can be observed that at W = 0.2 µm the $\boldsymbol{H}_x$, and $\boldsymbol{H}_y$ field contours are still confined into the Si guiding layer. The width of the primary guide, W is continuously reduced. At W less than 0.2 µm optical modes are no longer confined into the guiding layer, they have now expanded into the polymer layer. Fig. 8 (a) and (b), and Fig. 9 (a) and (b) show the field profile of $\boldsymbol{H}_x$ and $\boldsymbol{H}_y$ for the TE mode, and $\boldsymbol{H}_x$ and $\boldsymbol{H}_y$ for TM, respectively. It can be observed that the field profiles of the fundamental modes are quite close to that of the SMF. In this situation the modes are confined in the entire polymer region of the rib, which can be directly coupled to the SMF. The cross-section of the mode becomes W_1 x W_2 = 10 µm x 10 µm, and as the cross-sectional diameter of the SMF is approximately 12 µm successful coupling can be achieved.

The bound mode classifications of the transversal modes in the simulations were found using: TM: Hx >> Hy, Hz and TE: Hy >> Hx, Hz. The refractive index differences within the material structure ensure that the modes are confined into the guiding taper up to a certain value of W. These modes are oscillatory within the core region and exponentially decay in the substrate and cladding regions. After which point the mode is no longer simply confined into the primary guide

IV. Conclusion

The expansion of the spot-size contour is achieved by reducing the core dimension to a sufficiently small value. In the case of our results this occurred at W= 0.2 μm, where the primary guide could no longer support the mode, and thus radiating the mode into the surrounding layer. It has been demonstrated that the FEM for numerical analysis of the waveguide structure not only enables the accurate eigenmode solutions of simple waveguides but those of more complex geometries. The full vectorial modal solution has been employed to accurately determine the rib width where the mode expansion occurred. In particular, it has been shown that TE mode expands at a smaller width than TM. It has been demonstrated that to optimise the SSC a full vectorial numerical approach is necessary. High coupling efficiency has been demonstrated by matching filed profiles between the rib waveguide and the SMF. Further improvements of the tapered compactness and optimisation of its parameters are underway.

References

[1] B. Jalali, S. Yegnanarayanan, T. Yoon, T. Yoshimoto, I. Redina, and F. Coppinger, " Advances in Silicon-on-Insulator Optoelectronics" *J. Selected Topics in Quantum Electronics*, Vol. 4, no. 6, pp.938-947, 1998.

[2] T.Shoji, T.Tsuchizawa, T. Watanabe, K.Yamada and H. Morita,"Low Loss Mode Size Converter from 0.3μm Square Si Wire Waveguides to Single mode Fibres", *Electron. Lett*. vol. 38, no.25, Dec 2002.

[3] Regis S.Fan and R.Brian Hooker, "Tapered Polymer Single- Mode Waveguides for Mode Transformation", *J.Lightwave Technol*., vol.7, no.3, March 1999.

[4] B. M. A. Rahman, W. Boonthittanont, S. S. A. Obayya, T. Wongecharoen, E. O. Ladele, and K. T. V. Grattan, "Rigorous Beam Propagation Analysis of Tapered Spot-Size Converters in Deep-Etched Semiconductor Waveguides", *J.Lightwave Technol*., vol.21, no.12, December 2003.

[5] B. M. A. Rahman and S. Haxha, "Optimisation of microwave properties of ultrahigh-speed etched and unetched lithium niobate electrooptic modulators" *J.Lightwave Technol*., vol.20, 10, pp. 1856-1862, 2002.

[6] S. Haxha, B. M. Rahman, S. S. A. Obayya, and K. T. V. Grattan, "Velocity matching of GaAs electrooptic modulators" Applied Optics (LP) Vol. 42, 36, pp. 7179-7187, 2003.

Figure captions

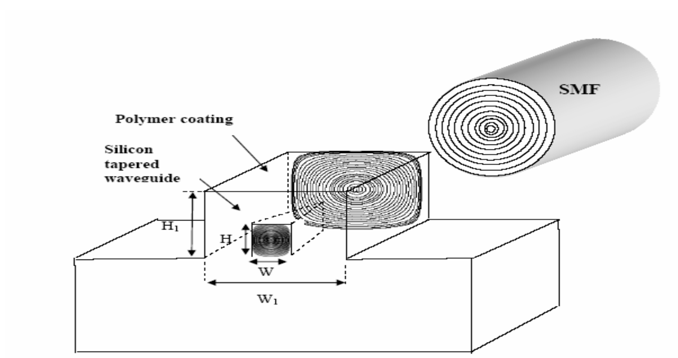

Fig. 1 Schematic diagram of the SSC.

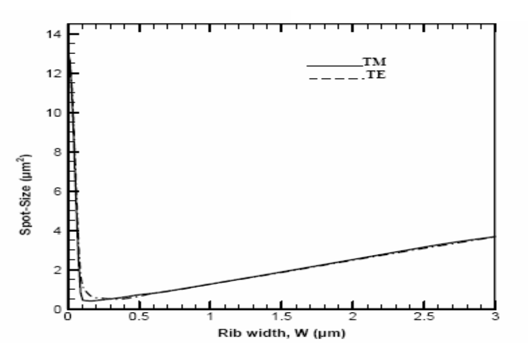

Fig. 2: Variation of the SS area as a function of the rib width.

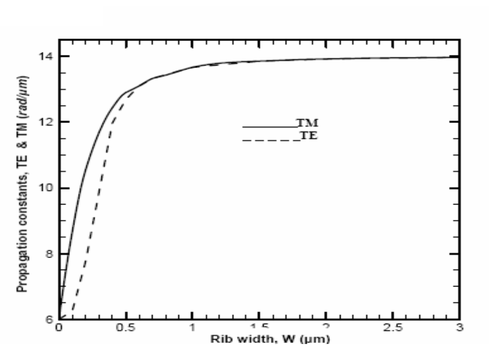

Fig. 2: Variation of the propagation constant as a function of the rib width.

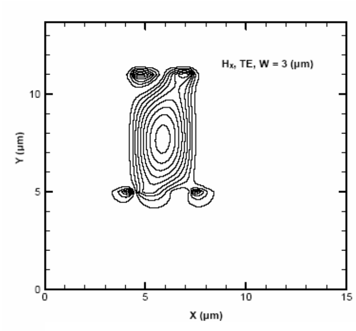

Fig. 4 (a): $\boldsymbol{H}_x$ field profile.

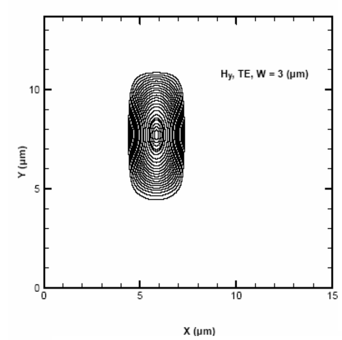

Fig. 4 (b): $\boldsymbol{H}_y$ field profile.

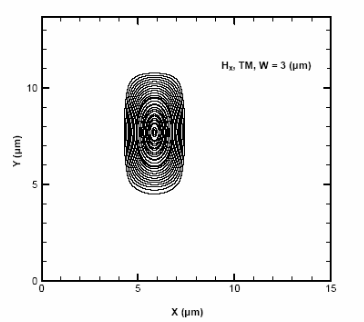

Fig. 5 (a): $\boldsymbol{H}_x$ field profile.

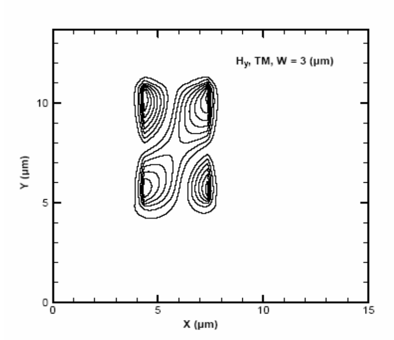

Fig. 5 (b): $\boldsymbol{H}_y$ field profile.

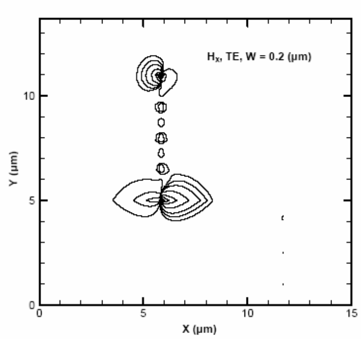

Fig. 6 (a): $\boldsymbol{H}_x$ field profile.

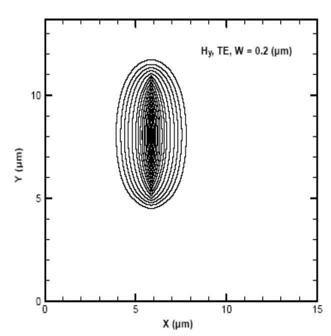

Fig. 6 (b): $\boldsymbol{H}_y$ field profile.

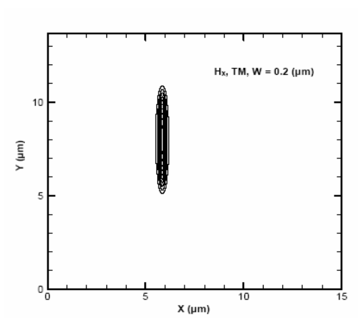

Fig. 7 (a): $\boldsymbol{H}_x$ field profile.

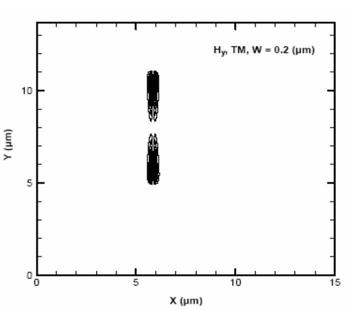

Fig. 7 (b): $\boldsymbol{H}_y$ field profile.

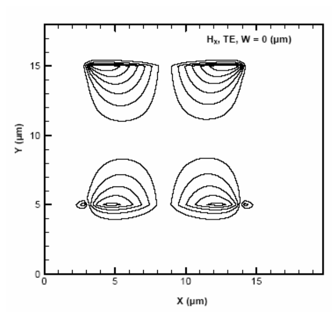

Fig. 8 (a): $\boldsymbol{H}_x$ field profile.

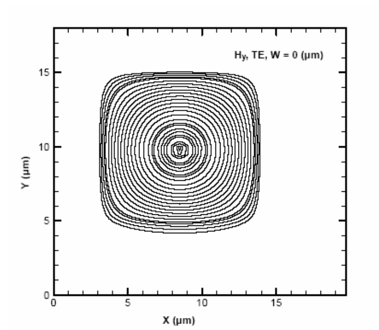

Fig. 9 (b): $\boldsymbol{H}_y$ field profile.

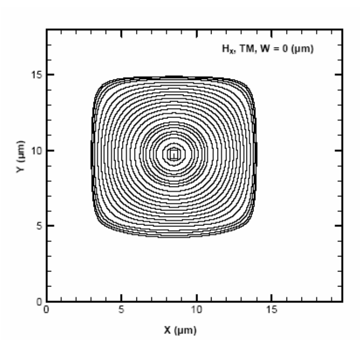

Fig. 9 (a): $\boldsymbol{H}_x$ field profile.

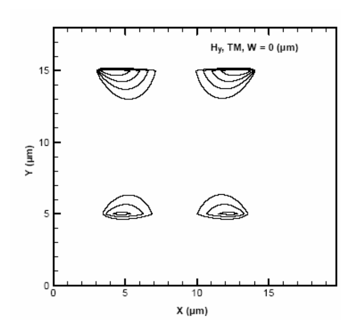

Fig. 9 (b): $\boldsymbol{H}_y$ field profile.